

 Open access • Journal Article • DOI:10.1049/IET-RSN.2016.0271

## **Multi-aspect micro-Doppler signatures for attitude-independent L/N quotient estimation and its application to helicopter classification** — [Source link](#)

Rui Zhang, Gang Li, Carmine Clemente, John J. Soraghan

**Published on:** 01 Apr 2017 - IET Radar Sonar and Navigation (Institution of Engineering and Technology)

**Topics:** Quotient

Related papers:

- [A Study of Complementary Filter Algorithm for Four-rotor Helicopters Attitude Control System](#)
- [Intelligent attitude and flapping angles estimation of flybarless helicopters under near-hover conditions](#)
- [Research on Attitude Estimation of Micro UAV Based on Sparse Line Optical Flow Field](#)
- [Design of Transfer Alignment for Micro-Inertial Attitude Measurement System Based on Distributed](#)
- [Sine Rotation Vector Method for Attitude Estimation of an Underwater Robot](#)

Share this paper:    

View more about this paper here: <https://typeset.io/papers/multi-aspect-micro-doppler-signatures-for-attitude-13haoifh9>

# Multi-Aspect Micro-Doppler Signatures for Attitude-Independent $L/N$ Quotient Estimation and its Application to Helicopter Classification

Rui Zhang<sup>1</sup>, Gang Li<sup>1\*</sup>, Carmine Clemente<sup>2</sup>, John J. Soraghan<sup>2</sup>

<sup>1</sup> Department of Electronic Engineering, Tsinghua University, Beijing, China

<sup>2</sup> Department of Electronic and Electrical Engineering, University of Strathclyde, 204 George Street, G1 1XW, Glasgow, UK

\*gangli@tsinghua.edu.cn

**Abstract:** Micro-Doppler signals returned from the main rotor of a helicopter can be used for feature extraction and helicopter classification. An intrinsic feature of a helicopter that may be extracted from the micro-Doppler signatures is the  $L/N$  quotient, where  $N$  denotes the number of rotor blades and  $L$  is the blade length. However, in monostatic radar, the  $L/N$  quotient cannot be accurately estimated due to the unknown attitude angles of non-cooperative helicopters. To solve this problem, an attitude-independent  $L/N$  quotient estimation method based on multi-aspect micro-Doppler signatures is proposed in this paper. The helicopter is observed from different aspect angles, and the multi-aspect micro-Doppler signatures are jointly processed to solve the attitude angles of the helicopter and estimate the  $L/N$  quotient unambiguously. Experiments with both simulated and real data demonstrate that, the proposed method is robust with respect to the attitude of the helicopter and, therefore, significantly improves the accuracy of  $L/N$  quotient estimation compared to only using the signature observed from single-aspect angle. This implies that the proposed method has the potential to increase the success rate of helicopter classification.

## 1. Introduction

Micro-Doppler signatures induced by the mechanical vibration or rotation of a target or its parts have been widely exploited for civil and military purposes [1-7]. In recent years, the problem of micro-Doppler-based helicopter classification has attracted much attention because of its application in air defence systems [8-18]. The  $L/N$  quotient, where  $N$  denotes the number of rotor blades and  $L$  is the blade length, is an intrinsic feature of a helicopter and has been widely used for helicopter classification. In [10-13], the authors developed the  $L/N$  quotient-based helicopter classification algorithm using monostatic radar. These methods can accurately identify the helicopter type in the assumption that the attitude of helicopter is horizontal. However, for non-cooperative helicopters with unknown attitudes, the methods in [10-13] suffer from performance degradation, because the  $L/N$  quotient solved by a monostatic radar is sensitive to the attitude of the helicopter. In practical applications, the main rotor of a helicopter has different attitudes due to the change of helicopter motion such as hovering, advancing and retreating [14, 15]. Therefore, the attitude-independent  $L/N$  quotient estimation is meaningful in practical scenarios and helpful to improve the robustness of existing algorithms of helicopter classification [16-19].

28 In order to overcome the limitation of monostatic radar, bistatic and multistatic radars have been  
29 employed to micro-Doppler-based target classification [20-29]. In [20-22], the motion parameters of  
30 vibrating/rotating targets were extracted based on analytical signal models in multistatic radar systems. In  
31 [23-26], the multistatic micro-Doppler signatures were used to overcome the self-occlusion of human  
32 target and obtain satisfactory classification results when the movement of the human target is away from  
33 the line of sight (LOS) of radar. However, these methods proposed in [23-26] cannot be straightforwardly  
34 applied in helicopter classification due to the distinct difference between the motion properties of  
35 helicopters and personnel targets. More specifically, the principal axis of a human is approximately  
36 perpendicular (when the human is walking or running) or parallel (when the human is crawling) to the  
37 ground, while the rotation axis of helicopter rotor has more variations in different helicopter motions such  
38 as hovering, advancing and retreating [14, 15].

39 Multistatic or multi-aspect micro-Doppler signatures of helicopter have attracted much attention in  
40 recent years [27-29]. In [27], the Global Navigation Satellite System (GNSS) is employed as the  
41 illuminator of a passive bistatic radar system to observe helicopters, and theoretical analysis and  
42 simulations demonstrate the effectiveness of this system for extracting helicopter signatures. In [28],  
43 multiple-input multiple-output (MIMO) radar is used to detect helicopters and the detection performance is  
44 effectively improved in comparison with monostatic radar. In [29], the authors formulated the signal  
45 model of the helicopter rotor in multistatic passive radars, which allow both estimation of helicopter  
46 parameters and inverse synthetic aperture radar (ISAR) imaging of the helicopter rotor. However, in  
47 existing literature, the effect of the attitude of the helicopter on the feature extraction has not been fully  
48 investigated yet.

49 In this paper, an attitude-independent  $L/N$  quotient estimation method is proposed based on multi-  
50 aspect micro-Doppler signatures. Based on the analytical relationship between the maximal micro-Doppler  
51 shift and the helicopter attitude, the attitude angles of the helicopter can be solved by analysing the micro-  
52 Doppler signatures collected from multiple aspect angles, and then the  $L/N$  quotient can be accurately  
53 retrieved and used for helicopter classification. Compared to the existing monostatic-based methods in  
54 [10-13] that do not consider the helicopter attitude, the proposed algorithm can provide satisfactory  
55 classification performance for non-cooperative helicopters with unknown attitudes.

56 The remainder of the paper is organized as follows. In Section 2, the background related to micro-  
57 Doppler signal model and helicopter classification is introduced. Then the proposed method is presented in  
58 detail in Section 3. Experimental results on synthetic and real data are given in Section 4 to validate the  
59 proposed method. Concluding remarks are provided in Section 5.

## 60 2. Background

### 61 2.1. Signal Model of Rotor Echo

62  
63 The helicopter's echoes are composed of the components reflected from its fuselage, rotating main  
64 rotor hub, main rotor and tail rotor [8, 9]. From the point of view of helicopter classification, the most  
65 useful information is provided by the structure of the rotating main rotor [12, 18], and the main rotor  
66 echoes can be separated from other components by using the method proposed in [18]. Supposing the  
67 parameters  $(N, \omega, L)$  represent the number of blades, the rotational speed and the blade length, respectively,  
68 the echoes from the main rotor can be expressed as [19]:

$$y(t_m) = \sigma L \exp\left(-j \frac{4\pi R_0}{\lambda}\right) \times \sum_{n=0}^{N-1} \text{sinc}[\Phi_n(t_m)] \exp[-j\Phi_n(t_m)], \quad m = 0, 1, \dots, M-1, \quad (1)$$

69 where

$$\Phi_n(t_m) = \frac{4\pi L}{\lambda} \sin \varphi_{rot,los} \times \cos\left(\omega t_m + \frac{2\pi n}{N} + \theta\right), \quad (2)$$

70  $\lambda$  is the carrier wavelength of the radar system,  $t_m$  denotes the sampling instant with the sampling  
71 frequency  $f_s$ ,  $M$  is the number of samples,  $\text{sinc}(x) = \sin(x)/x$ ,  $R_0$  is the range between the helicopter and the  
72 radar,  $\sigma$  is the equivalent scattering coefficient of the main rotor, and  $\Phi_n(t_m)$  denotes the phase of the echo  
73 corresponding to the  $n$ -th blade,  $\theta$  denotes the initial phase of the received signal,  $\varphi_{rot,los}$  is the angle  
74 formed by the rotation axis and the LOS direction. In (2), the sine of angle  $\varphi_{rot,los}$  follows

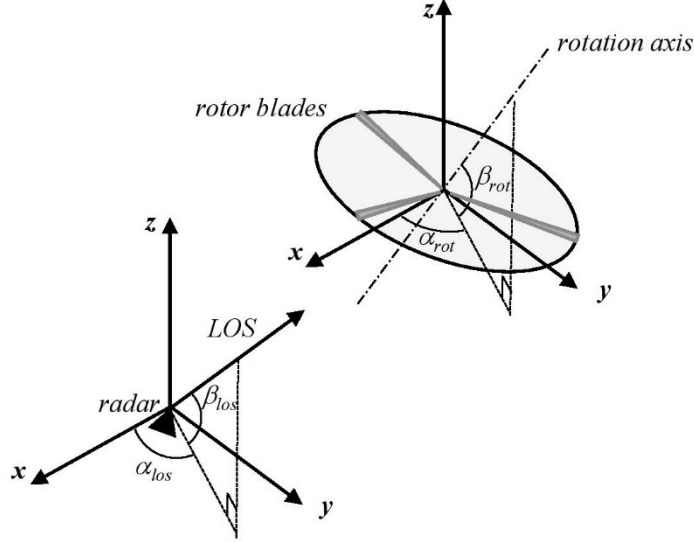
$$\sin \varphi_{rot,los} = \sqrt{1 - \langle \boldsymbol{\eta}_{rot}, \boldsymbol{\eta}_{los} \rangle^2}, \quad (3)$$

75 where the vector  $\boldsymbol{\eta}_{rot}$  denotes the direction of the rotation axis,  $\boldsymbol{\eta}_{los}$  denotes the LOS direction, and  $\langle \cdot, \cdot \rangle$   
76 denotes the inner product. The geometry of radar observation is shown in Fig. 1, where  $\alpha_{rot}$  and  $\beta_{rot}$  denote  
77 the azimuth angle and the pitch angle of  $\boldsymbol{\eta}_{rot}$ , respectively,  $\alpha_{los}$  and  $\beta_{los}$  denote the azimuth angle and the  
78 pitch angle of  $\boldsymbol{\eta}_{los}$ , respectively. Then  $\boldsymbol{\eta}_{rot}$  and  $\boldsymbol{\eta}_{los}$  can be expressed as

$$\boldsymbol{\eta}_{rot} = (\cos \alpha_{rot} \cos \beta_{rot}, \sin \alpha_{rot} \cos \beta_{rot}, \sin \beta_{rot}), \quad (4)$$

$$\boldsymbol{\eta}_{los} = (\cos \alpha_{los} \cos \beta_{los}, \sin \alpha_{los} \cos \beta_{los}, \sin \beta_{los}). \quad (5)$$

79 In practical scenarios, the LOS angles  $(\alpha_{los}, \beta_{los})$  can be obtained from system configuration or  
80 estimated by using signal processing techniques [30], but the attitude angles  $(\alpha_{rot}, \beta_{rot})$  of non-cooperative  
81 helicopters are unknown [14, 15]. Since the micro-Doppler signatures are influenced by the helicopter  
82 attitude, it is very meaningful to develop attitude-independent algorithms of helicopter feature extraction  
83 in practical scenarios.



84  
85 **Fig. 1.** Geometry of a radar and a 3-blade rotor.  
86

87 **2.2.  $L/N$  Quotient-based Classification Scheme**  
88

89 The  $L/N$  quotient-based algorithm is one of the most widely used methods for helicopter classification  
90 [10-13]. In this subsection, the theoretical foundation of this method is briefly reviewed, and its limitation  
91 in monostatic scenario is also analysed.

92 It is clear from (1) and (2) that the received signal is periodic and the period is

$$T = \frac{2\pi}{N\omega}. \quad (6)$$

93 The instantaneous frequency corresponding to the  $n$ -th blade can be directly obtained by taking the time  
94 derivative of  $\Phi_n(t)$ :

$$\begin{aligned} f_{md,n}(t_m) &= \frac{1}{2\pi} \times \frac{d\Phi_n(t)}{dt} \\ &= -\frac{2}{\lambda} \omega L \sin \varphi_{rot,los} \times \sin \left( \omega t_m + \frac{2\pi n}{N} + \theta \right), \end{aligned} \quad (7)$$

95 It is obvious from (7) that the maximal Doppler shift of the received signal is

$$f_{md,max} = \frac{2}{\lambda} \omega L \sin \varphi_{rot,los}. \quad (8)$$

96 According to (6) and (8), the  $L/N$  quotient can be calculated as

$$\begin{aligned} \frac{L}{N} &= \frac{\lambda}{4\pi} \times \frac{Tf_{md,max}}{\sin \varphi_{rot,los}} \\ &= \frac{\lambda}{4\pi} \times \frac{Tf_{md,max}}{\sqrt{1 - \langle \mathbf{n}_{rot}, \mathbf{n}_{los} \rangle^2}}. \end{aligned} \quad (9)$$

where the period  $T$  and maximal Doppler shift  $f_{md,max}$  can be extracted from the micro-Doppler signals. Since  $L/N$  quotient is an intrinsic characteristic of a helicopter, most helicopters can be identified according to their  $L/N$  quotient values [16].

In monostatic-based algorithm, no information about the helicopter attitude can be obtained and the helicopter pitch angle  $\beta_{rot}$  is assumed to be  $90^\circ$ . As a result, the  $L/N$  quotient is regarded as

$$\left(\frac{L}{N}\right)_{mono} = \frac{\lambda}{4\pi} \times \frac{Tf_{md,max}}{\cos \beta_{los}}. \quad (10)$$

It is obvious that formula (10) is different from (9), and the estimated  $(L/N)_{mono}$  will deviate from the real value of  $L/N$  quotient when the helicopter attitude is not horizontal. That is to say, the monostatic-based algorithm cannot accurately estimate the  $L/N$  quotient of non-cooperative helicopters with unknown attitudes.

**Table 1** The parameters in the example in Section 2.2

Carrier frequency $f_c$	900 MHz
Sampling frequency $f_s$	6 KHz
Sampling number $M$	2400
Rotor attitude angles $(\alpha_{rot}, \beta_{rot})$	$(60^\circ, 75^\circ)$
LOS angles $(\alpha_{los}, \beta_{los})$	$(0^\circ, 40^\circ)$

**Table 2** The parameters of helicopter.

Type	$N$	$L$ (m)	$\omega$ (rps)	$L/N$	* range of $\beta_{rot}$
AH-1 Cobra	2	7.32	4.9	3.66	$[74^\circ, 106^\circ]$
AH-64 Apache	4	7.32	4.8	1.83	$[60^\circ, 120^\circ]$
UH-60 Black Hawk	4	8.18	4.3	2.05	$[60^\circ, 120^\circ]$
AS332 Super Puma	4	7.80	4.4	1.95	$[74^\circ, 106^\circ]$
A109 Agusta	4	5.50	6.4	1.38	$[77^\circ, 103^\circ]$
SA365 Dauphin	4	5.97	5.8	1.49	$[75^\circ, 105^\circ]$

\* The ranges of  $\beta_{rot}$  are found in the pilot's books of corresponding helicopters.

To explain the failure of monostatic  $L/N$  quotient estimation for non-horizontal helicopters, we analyse the micro-Doppler signature of an AH-64 Apache helicopter with the following simulation. The simulation parameters and the parameters of AH-64 Apache helicopter are listed in Table 1 and Table 2, respectively. With the monostatic  $L/N$  quotient estimation algorithm, the value of  $(L/N)_{mono}$  is calculated as 1.658 when the pitch angle  $\beta_{rot}$  of the rotation axis is  $75^\circ$ , i.e., when the helicopter rotor deviates from the horizontal attitude with  $15^\circ$ . It is clear that  $(L/N)_{mono}$  has deviated from the real value of  $L/N$ , i.e. 1.830. Considering that the  $L/N$  quotient of SA365 Dauphin helicopter (another helicopter type) is 1.490, the AH-

64 Apache with  $\beta_{rot} = 75^\circ$  may be mistakenly identified as a SA365 Dauphin by using monostatic  $L/N$  quotient estimation according to the nearest neighbour rule.

### 3. Proposed method

In order to accomplish attitude-independent classification of non-cooperative helicopters, in this section we propose a multi-aspect micro-Doppler-based algorithm for  $L/N$  quotient estimation. The block diagram of the proposed method is depicted in Fig. 2. It can be seen that the proposed method can be divided into two stages: 1) monostatic micro-Doppler analysis; 2) Multi-aspect micro-Doppler analysis. The procedures of Stages 1 and 2 are presented in details in the following subsections.

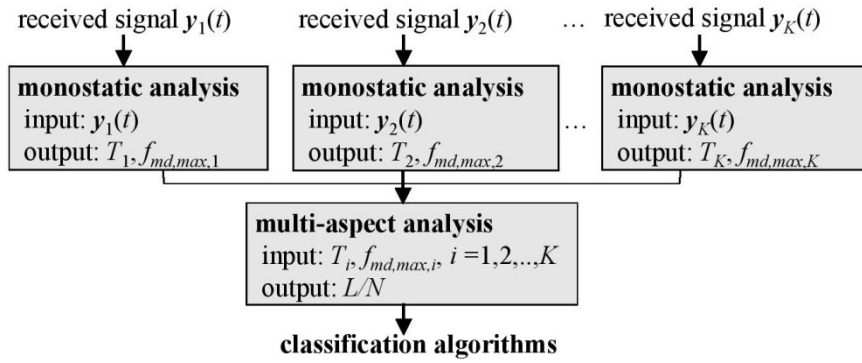


Fig. 2. The block diagram of the proposed method.

#### 3.1. Monostatic Micro-Doppler Analysis

At this stage, the received signal obtained from each aspect is processed separately, and the period  $T_i$  and maximal Doppler shift  $f_{md,max,i}$  are extracted via monostatic micro-Doppler analysis, where the subscript  $i$  indicates the index of aspect. The authors of [10-19] presented a number of effective methods for monostatic micro-Doppler analysis. In this paper, the period  $T_i$  is estimated by using the autocorrelation function of the received signal as presented in [18]. Then, the initial phase  $\theta$  of the received signal is synchronized to be  $\pi/2$  by using the method proposed in [19]. After the previous processing, the signal model in (1) can be rewritten as

$$y_{N,f_{md,max}}(t_m) = C \times \sum_{n=0}^{N-1} \left\{ \text{sinc} \left\{ -TNf_{md,max} \sin \left[ \frac{2\pi}{N} \left( \frac{t_m}{T} + n \right) \right] \right\} \times \exp \left\{ jTNf_{md,max} \sin \left[ \frac{2\pi}{N} \left( \frac{t_m}{T} + n \right) \right] \right\} \right\}, \quad (11)$$

where  $C$  is a constant, and the rotational speed  $\omega$  is replaced with  $2\pi/NT$  according to (6).

For each parameter pair  $(N, f_{md,max}) \in \{2,3,\dots,7\} \otimes (0, f_s/4]$ , the following correlation coefficient measures the relevancy between the model  $y_{N,f_{md,max}}(t_m)$  and the received signal  $y(t_m)$ :

$$c_{N, f_{md, \max}} = \frac{\sum_{m=0}^{M-1} y_{N, f_{md, \max}}(t_m) y^*(t_m)}{\sqrt{\sum_{m=0}^{M-1} |y_{N, f_{md, \max}}(t_m)|^2 \sum_{m=0}^{M-1} |y(t_m)|^2}}, \quad (12)$$

Based on the Maximum Likelihood (ML) analysis presented in [18], the maximal Doppler shift  $f_{md, \max}$  can be estimated as:

$$f_{md, \max} = \arg \max_{f_{md, \max} \leq f_s/4} \left\{ \max_{N \in \{2, 3, \dots, 7\}} c_{N, f_{md, \max}} \right\}. \quad (13)$$

It is worth emphasizing that the maximal Doppler shift  $f_{md, \max}$  can be properly extracted according to (14) without a priori information about the number of blades  $N$ . We refer readers to literature [18] for more details about this maximum likelihood estimation.

### 3.2. The Multi-Aspect Micro-Doppler Analysis Algorithm

At this stage, the attitude angles  $(\alpha_{rot}, \beta_{rot})$  are determined by using the maximal Doppler shift  $f_{md, \max, i}$  and the LOS angles  $(\alpha_{los, i}, \beta_{los, i})$  ( $i = 1, 2, \dots, K$ ). Then, with the estimated attitude angles  $(\alpha_{rot}, \beta_{rot})$ , we can calculate the  $L/N$  quotient according to (9). The multi-aspect micro-Doppler analysis at this stage accomplishes attitude-independent  $L/N$  quotient estimation, which has not been investigated in existing literature yet.

It is clear from (8) that the maximal Doppler shift  $f_{md, \max}$  is proportional to the following three factors: 1) the velocity of the blade tip, i.e.  $\omega L$ ; 2) the reciprocal of the wave length, i.e.  $1/\lambda$ ; and 3) the sine value  $\sin \varphi_{rot, los}$ . Supposing that the helicopter is observed from  $K$  different aspects, the maximal Doppler shifts corresponding to Aspect  $i$  and Aspect  $j$  satisfy the following relationship according to (8):

$$\frac{f_{md, \max, i}}{f_{md, \max, j}} = \frac{\sin \varphi_{rot, los, i} / \lambda_i}{\sin \varphi_{rot, los, j} / \lambda_j}, \quad (i, j = 1, 2, \dots, K.) \quad (14)$$

where  $\varphi_{rot, los, i}$  denotes the included angle formed by rotation axis of the helicopter rotor and the LOS of Aspect  $i$ . To avoid zero term at denominator in (15), which corresponds to the case that the LOS is perpendicular to the rotor plane, (15) is rewritten as:

$$\frac{f_{md, \max, i}}{\sum_{j=1}^K f_{md, \max, j}} = \frac{\sin \varphi_{rot, los, i} / \lambda_i}{\sum_{j=1}^K \sin \varphi_{rot, los, j} / \lambda_j}. \quad (i = 1, 2, \dots, K.) \quad (15)$$

In (16), the micro-Doppler shifts  $f_{md, \max, i}$  ( $i = 1, 2, \dots, K$ ) have been estimated in Stage 1, the angle  $\varphi_{rot, los, i}$  is determined by  $(\alpha_{los, i}, \beta_{los, i})$  and  $(\alpha_{rot}, \beta_{rot})$ , where  $(\alpha_{los, i}, \beta_{los, i})$  are known and  $(\alpha_{rot}, \beta_{rot})$  are unknown. Based on (16), a group of constraint equations containing  $(\alpha_{rot}, \beta_{rot})$  are obtained. Since there



are two independent unknown angles, i.e.,  $\alpha_{rot}$  and  $\beta_{rot}$ , at least two independent constraint equations are needed to determine them. Therefore, the helicopter should be observed from at least three aspects, i.e.,  $K \geq 3$ .

It is difficult to find the analytical solution of (16). Here we solve the values of  $(\alpha_{rot}, \beta_{rot})$  by full search. We uniformly divide the attitude angles domain that  $(\alpha_{rot}, \beta_{rot})$  belong in into  $P \times Q$  discrete values, i.e.  $\alpha_{rot} \in \{\alpha_1, \alpha_2, \dots, \alpha_P\}$  and  $\beta_{rot} \in \{\beta_1, \beta_2, \dots, \beta_Q\}$ , and compute the sine value  $\sin \varphi_{rot,los,i}$  according to (3)-(5) for each pair of  $(\alpha_{rot}, \beta_{rot})$ . Based on (16), the value of  $(\alpha_{rot}, \beta_{rot})$  is searched by

$$(\alpha'_{rot}, \beta'_{rot}) = \arg \max_{(\alpha_{rot}, \beta_{rot})} X_K(\alpha_{rot}, \beta_{rot}), \quad (16)$$

where

$$X_K(\alpha_{rot}, \beta_{rot}) = \sum_{i=1}^K \left( \frac{\sin[\varphi_i(\alpha_{rot}, \beta_{rot})]/\lambda_i - \frac{f_i}{\sum_{j=1}^K \sin[\varphi_j(\alpha_{rot}, \beta_{rot})]/\lambda_j} - \frac{f_i}{\sum_{j=1}^K f_j}} \right)^{-2}, \quad (17)$$

where the number of observation  $K$  is not less than 3 as analyzed above.

With the estimated  $(\alpha_{rot}, \beta_{rot})$ , the  $L/N$  quotient can be calculated according to (9):

$$\left( \frac{L}{N} \right)_{multi,K} = \frac{1}{K} \sum_{i=1}^K \frac{\lambda_i T_i f_{md,max,i}}{4\pi \sin \varphi_{rot,los,i}}, \quad (18)$$

where  $T_i$  have been estimated at Stage 1. It is clear from (19) that the  $L/N$  quotient is calculated by averaging over  $K$  radar nodes, therefore, the estimation accuracy of  $(L/N)_{multi,K}$  is expected to be improved as the number of aspects angles  $K$  increases.

Based on the above description, the proposed algorithm for  $L/N$  quotient estimation is summarized below:

---

**Algorithm:** Attitude-indepent  $L/N$  quotient estimation based on multi-aspect micro-Doppler signatures

**Input:**  $y_1(t), y_2(t), \dots, y_K(t)$ , i.e., the received signals observed from  $K$  different aspects.

**Stage 1:** monostatic micro-Doppler analysis. Do Steps 1-1, 1-2 and 1-3, for  $i=1, 2, \dots, K$ .

**Step 1-1:** Synchronize  $y_i(t)$  at the first flash instant.

**Step 1-2:** Estimate the period  $T_i$  of signal  $y_i(t)$  by using its autocorrelation function.

**Step 1-3:** Estimate the maximal micro-Doppler shift  $f_{md,max,i}$  of signal  $y_i(t)$  by maximum likelihood method.

**Stage 2:** multi-aspect micro-Doppler analysis.

187 **Step 2-1:** Calculate attitude angles  $(\alpha_{rot}, \beta_{rot})$  by using  $f_{md,max,i}$  ( $i=1,2,\dots, K$ ) according to (17)  
 188 and (18).

189 **Step 2-2:** Calculate  $L/N$  quotient according to (19).

190 **Output:** The  $L/N$  quotient.

191  
 192 In what follows, we use the proposed method to analyse the simulated signal from an AH-64 Apache  
 193 helicopter which has been described in Section 2.2. The configuration of the radar system and the  
 194 helicopter parameters are listed in Table 1. Now we assume that the helicopter is observed from three  
 195 aspects as listed in Table 3.

196 **Table 3** The LOS angles in simulation in Section 3.2  
 197

	$\alpha_{los,i}$	$\beta_{los,i}$
Aspect 1	0°	40°
Aspect 2	50°	50°
Aspect 3	90°	60°

198 **Table 4** Results of monostatic analysis in Simulation in Section 3.2  
 199

	$T_i$ (ms)	$f_{md,max,i}$ (Hz)
estimate from Aspect 1	52.2	919
estimate from Aspect 2	52.2	567
estimate from Aspect 3	52.2	419

200  
 201 With the algorithms described in Section 3.1, the period and maximal Doppler shift of the received  
 202 signal from each aspect are extracted separately, and the results are listed in Table 4. It can be seen that,  
 203 the estimation of the period  $T_i$  ( $i=1,2,3$ ) is not influenced by the change of the aspect angle, while the  
 204 maximal micro-Doppler shift  $f_i$  ( $i=1,2,3$ ) varies with the different aspect angles.

205 With the estimated  $f_{md,max,i}$  and the known  $(\alpha_{los,i}, \beta_{los,i})$  ( $i=1,2,3$ ), the function  $X_3(\alpha_{rot}, \beta_{rot})$  is  
 206 computed according to (18) and the search result in  $(\alpha_{rot}, \beta_{rot})$  domain is depicted in Fig. 3. It is clear that  
 207 the peak of  $X_3(\alpha_{rot}, \beta_{rot})$ , i.e.  $(60^\circ, 75^\circ)$ , is located at the real value of  $(\alpha_{rot}, \beta_{rot})$ . With the estimated  $(\alpha_{rot},$   
 208  $\beta_{rot})$ , the  $L/N$  quotient is calculated according to (19), and the result is 1.827, which is very close to the real  
 209 value of  $L/N$ , i.e., 1.830. The estimation error in noise free case is caused by the quantization error in  
 210 searching process and its influence to the classification results is neglectable in most cases. This  
 211 simulation depicts the processing procedures of the proposed method and verifies the effectiveness of this  
 212 method. The performance of the proposed method will be evaluated in detail in Section 4.

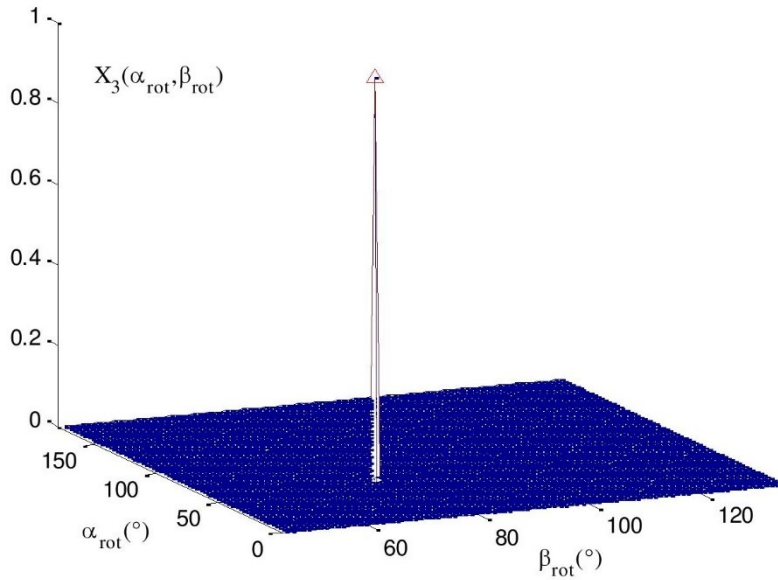


**Fig. 3.** The distributions of  $X_3(\alpha_{rot}, \beta_{rot})$ . The red triangle indicates the true values of  $(\alpha_{rot}, \beta_{rot})$ .

### 3.3. Discussions

**3.3.1 Discussions about the Ranges of Related Angles:** In this subsection, the search domain of  $(\alpha_{rot}, \beta_{rot})$  and the value ranges of  $(\alpha_{los,i}, \beta_{los,i})$  in optimization problem (17) are discussed. Each type of helicopter has its own limitation of pitch angle  $\beta_{rot}$ , and the allowable range of  $\beta_{rot}$  can be found in its pilot's handbook. It can be seen from Table 2 that the deviation of pitch angle  $\beta_{rot}$  from  $90^\circ$  is less than  $30^\circ$ . Therefore, we set the search range of  $\beta_{rot}$  to be  $[60^\circ, 120^\circ]$  in (17). Since the azimuth angle  $\alpha_{rot}$  of helicopter rotor varies from  $0^\circ$  to  $180^\circ$ , and the azimuth angles between  $180^\circ$  and  $360^\circ$  are equivalent to those between  $0^\circ$  and  $180^\circ$  due to the symmetry of helicopter rotor, we set the search range of  $\alpha_{rot}$  to be  $[0^\circ, 180^\circ]$ . The range of the pitch angle  $\beta_{los,i}$  of the LOS depends on application scenarios. In this paper, the performance of the proposed method is investigated under the following two scenarios: 1) Small pitch angle, i.e.  $\beta_{los,i} \in [0^\circ, 3^\circ]$ . This scenario is corresponding to applications of classifying helicopters at a remote distance. 2) Wide range of pitch angle, i.e.  $\beta_{los,i} \in [0^\circ, 70^\circ]$ . This corresponds to more general scenarios. For example, in applications of classifying unmanned micro-Drones in city scenarios [32], the pitch angle of radar LOS can be much larger than  $3^\circ$ . In addition, the azimuth angle  $\alpha_{los,i}$  of radar LOS varies between  $0^\circ$  and  $360^\circ$ . In conclusion, the search domain of optimization problem (17) is  $(\alpha_{rot}, \beta_{rot}) \in [0^\circ, 180^\circ] \otimes [60^\circ, 120^\circ]$ , and the value range of  $(\alpha_{los,i}, \beta_{los,i})$  is  $[0^\circ, 360^\circ] \otimes [0^\circ, 3^\circ]$  (in Scenario 1) or  $[0^\circ, 360^\circ] \otimes [0^\circ, 70^\circ]$  (in Scenario 2).

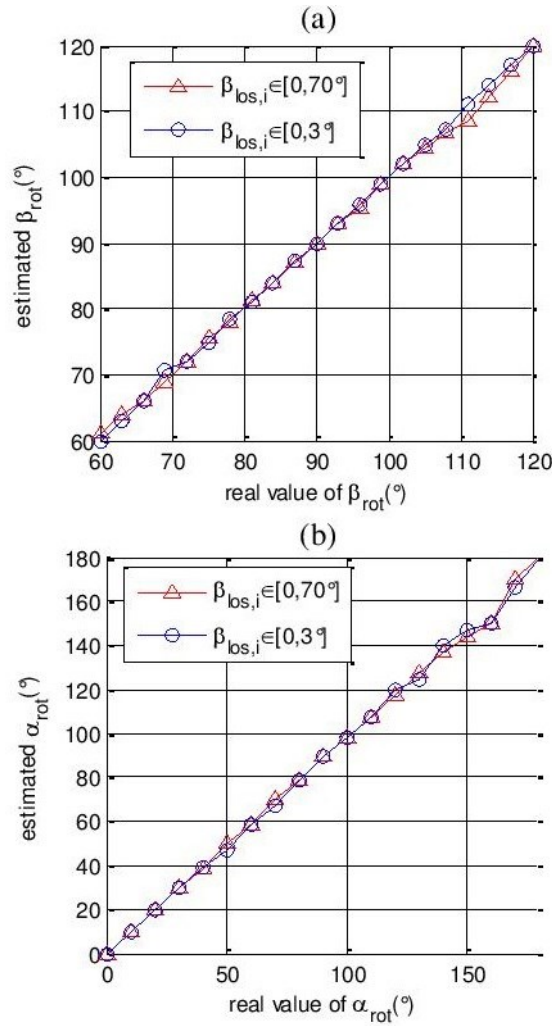


**Fig. 4.** The angles  $(\alpha_{\text{rot}}, \beta_{\text{rot}})$  estimated by the proposed method versus their real values.

a estimated  $\beta_{\text{rot}}$  versus real value of  $\beta_{\text{rot}}$ .

b estimated  $\alpha_{\text{rot}}$  versus real value of  $\alpha_{\text{rot}}$ .

**3.3.2 Discussions about the Optimization Problem (17):** As presented in Section 3.2, the solution of (17) is obtained by full search within search domain of  $(\alpha_{\text{rot}}, \beta_{\text{rot}})$ . In the searching process, as the angles  $(\alpha_{\text{rot}}, \beta_{\text{rot}})$  approach their real values, every term at the right side of (18) approaches  $+\infty$ . Therefore, the values of  $(\alpha_{\text{rot}}, \beta_{\text{rot}})$  can be found by searching the maximum of (17). To evaluate the properties of the optimization problem (17) throughout the search domain of  $(\alpha_{\text{rot}}, \beta_{\text{rot}})$ , we perform the following simulations with parameters of AH-64 Apache. First, the value of  $\beta_{\text{rot}}$  is selected from  $60^\circ$  to  $120^\circ$  with a step size of  $3^\circ$ , and the angles  $\alpha_{\text{rot}}$ ,  $\alpha_{\text{los},i}$  and  $\beta_{\text{los},i}$  are randomly selected from  $[0^\circ, 180^\circ]$ ,  $[0^\circ, 360^\circ]$  and  $[0^\circ, 3^\circ]$  (in Scenario 1) or  $[0^\circ, 70^\circ]$  (in Scenario 2), respectively. Under each value of  $\beta_{\text{rot}}$ , we perform 50 trials of simulations, and the value of estimated  $\beta_{\text{rot}}$  is averaged over 50 trials. The relative error of  $\beta_{\text{rot}}$ , which is defined as the absolute estimation error of  $\beta_{\text{rot}}$  normalized by its real value, is averaged over all trials. The

simulation results are depicted in Fig. 4 (a) and table 5, and the results show that angle  $\beta_{rot}$  can be accurately estimated throughout the value range of  $\beta_{rot}$ . Then, similar simulations are performed to evaluate the estimation accuracy of azimuth angle  $\alpha_{rot}$ . The azimuth angle  $\alpha_{rot}$  is selected from  $0^\circ$  to  $180^\circ$  with a step size of  $10^\circ$ , and the angles  $\beta_{rot}$ ,  $\alpha_{los,i}$  and  $\beta_{los,i}$  are randomly selected from  $[60^\circ, 120^\circ]$ ,  $[0^\circ, 360^\circ]$  and  $[0^\circ, 3^\circ]$  (in Scenario 1) or  $[0^\circ, 70^\circ]$  (in Scenario 2), respectively. Simulation results depicted in Fig. 4 (b) and Table 5 confirm the effectiveness of the proposed method for estimating  $\alpha_{rot}$ . The relative error of  $\alpha_{rot}$  is larger than that of  $\beta_{rot}$ , this is because function (18) is more sensitive to the value of  $\beta_{rot}$ .

**Table 5** The relative errors of  $(\alpha_{rot}, \beta_{rot})$

	Scenario 1 $\beta_{los,i} \in [0^\circ, 3^\circ]$	Scenario 2 $\beta_{los,i} \in [0^\circ, 70^\circ]$
relative error of $\beta_{rot}$	0.28%	0.97%
relative error of $\alpha_{rot}$	3.22%	2.95%

## 4. Simulations and Experimental Results

In this section, we evaluate the proposed algorithm with both simulated and real data.

### 4.1. Influence of the Helicopter Attitude on $L/N$ Quotient Estimation in Noise-free Case

As presented in Section 2.2, the monostatic  $L/N$  quotient estimation algorithm fails to identify helicopters when the rotor of helicopter deviates from horizontal attitude. In contrast, the proposed method is capable of attitude-independent  $L/N$  quotient estimation. In this simulation, the performances of the proposed method and the monostatic  $L/N$  quotient estimation are tested under different helicopter attitudes.

The carrier frequency  $f_c$  of radar is set to be 900 MHz. The sampling frequency  $f_s$  and signal length  $M$  are set to be 6000 Hz and 2400 points, respectively. Six types of helicopters are considered and their parameters are listed in Table 2. The helicopter is observed from three different aspects. The azimuth angles  $\alpha_{los,i}$  ( $i = 1,2,3$ ) of the LOS are randomly selected from  $[0^\circ, 360^\circ]$  with equal probability. The pitch angles  $\beta_{los,i}$  ( $i = 1,2,3$ ) of the LOS are configured under the following two scenarios: 1) Small pitch angle, i.e. angles  $\beta_{los,i}$  ( $i = 1,2,3$ ) are selected from  $[0^\circ, 3^\circ]$  with equal probability. 2) Wide range of pitch angle, i.e. angles  $\beta_{los,i}$  ( $i = 1,2,3$ ) are selected from  $[0^\circ, 70^\circ]$  with equal probability. The azimuth angle  $\alpha_{rot}$  of the rotor is randomly selected from  $[0^\circ, 180^\circ]$  with equal probability, and the pitch angle  $\beta_{rot}$  is set to vary from  $75^\circ$  to  $105^\circ$  with a step size of  $2.5^\circ$ . For each value of  $\beta_{rot}$ , the proposed method and the monostatic  $L/N$  quotient estimation algorithm are repeated for 100 trials for each type of helicopter. In this simulation, no noise is added to the signal.

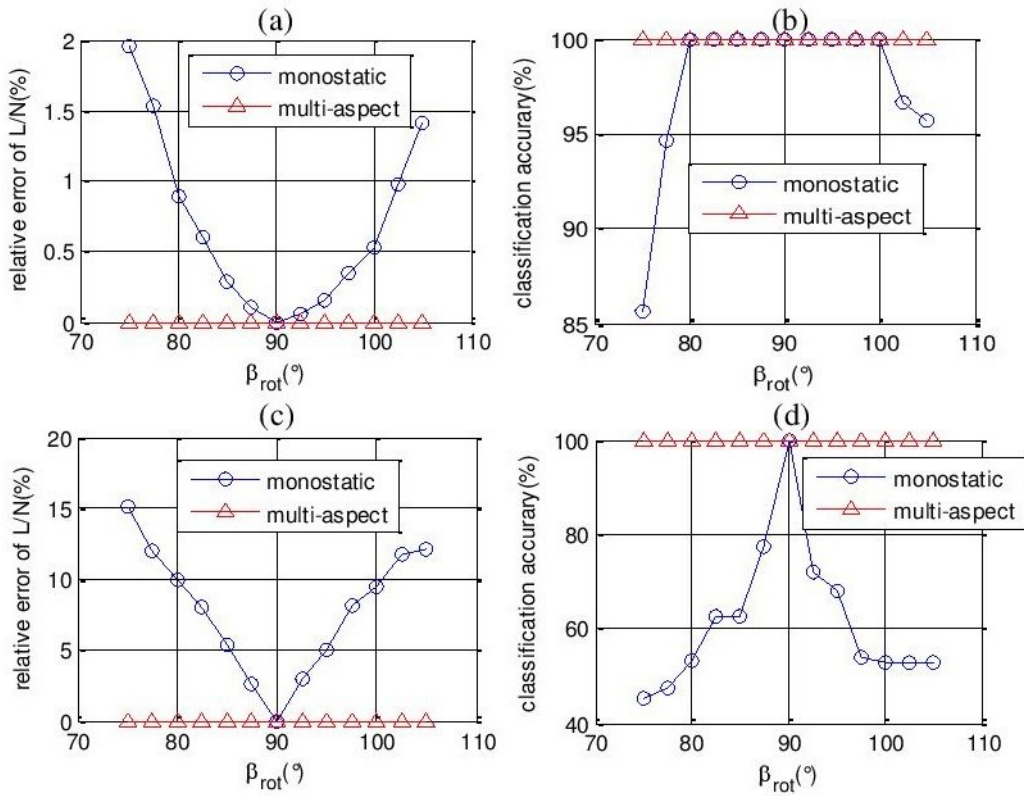


**Fig. 5.** The performances of the proposed method and the monostatic algorithm under different helicopter attitudes.  
a The relative estimation error of  $L/N$  quotient versus angle  $\beta_{rot}$  when  $\beta_{los,i} \in [0^\circ, 3^\circ]$ .  
b The classification accuracy versus angle  $\beta_{rot}$  when  $\beta_{los,i} \in [0^\circ, 3^\circ]$ .  
c The relative estimation error of  $L/N$  quotient versus angle  $\beta_{rot}$  when  $\beta_{los,i} \in [0^\circ, 70^\circ]$ .  
d The classification accuracy versus angle  $\beta_{rot}$  when  $\beta_{los,i} \in [0^\circ, 70^\circ]$ .

The averaged relative estimation error of  $L/N$  quotient and the classification accuracy versus  $\beta_{rot}$  are depicted in Fig. 5, respectively. In this paper, the classification accuracy is defined as the percentage of trials in which the helicopters are correctly classified. It is clear from Fig. 5 that the proposed method can accurately estimate the  $L/N$  quotient and successfully classify helicopters under each angle  $\beta_{rot}$  in both Scenario 1 and Scenario 2. In comparison, monostatic algorithm suffers different degrees of performance degradation in Scenarios 1 and 2. In Scenario 1, the estimation error of  $L/N$  quotient yielded by the monostatic algorithm is quite slight, and the classification accuracy of monostatic algorithm decreases mildly when  $\beta_{rot}$  deviates beyond  $[80^\circ, 100^\circ]$ . In Scenario 2, the performance of monostatic algorithm degrades obviously when  $\beta_{rot}$  deviates from  $90^\circ$ . Therefore, the proposed method have advantages over monostatic methods, especially when  $\beta_{rot}$  deviates obviously from  $90^\circ$  or the pitch angle of the LOS is not too small.

293 Allowing for that the deviation of angle  $\beta_{rot}$  from  $90^\circ$  can be as large as  $30^\circ$  for certain helicopter  
 294 such as AH-64 Apache, and the LOS angles  $\beta_{los,i}$  can be much larger than  $3^\circ$  in some applications [32], the  
 295 multi-aspect deployment is justified in realistic scenarios.

#### 296 4.2. The Performance of the Proposed Method in Noisy Conditions

297 In this simulation, the maximal Doppler  $f_{md,max,i}$  and the period  $T_i$  are estimated in noisy conditions,  
 298 and the performance of the proposed method is tested under different noise levels.

299 **Table 6** The angle parameters in Simulation 4.2.

$\alpha_{los,i}$	randomly selected from $[0^\circ, 360^\circ]$ with equal probability
$\beta_{los,i}$	Scenario 1: randomly selected from $[0^\circ, 3^\circ]$ with equal probability Scenario 2: randomly selected from $[0^\circ, 70^\circ]$ with equal probability
$\alpha_{rot}$	randomly selected from $[0^\circ, 180^\circ]$ with equal probability
$\beta_{rot}$	randomly selected from corresponding range stipulated in the pilot's handbook as depicted in Table 2

300  
 301 The carrier frequency  $f_c$  of radar is set to 900 MHz. The sampling frequency  $f_s$  and signal length  $M$   
 302 are set to be 6000 Hz and 2400 points, respectively. Six types of helicopters are considered and their  
 303 parameters are listed in Table 2. The helicopter is observed from  $K$  ( $K=3$  or  $4$ ) different aspects, the LOS  
 304 angles ( $\alpha_{los,i}, \beta_{los,i}$ ) and attitude angles ( $\alpha_{rot}, \beta_{rot}$ ) are randomly selected from their definition domains as  
 305 depicted in Table 6. The SNR is set to vary from -5dB to 10dB with a step size of 5dB. Under each SNR,  
 306 the algorithm is tested with 120 Monte Carlo trails.

307 The relative estimation error of  $L/N$  quotient and the classification accuracy are depicted in Fig. 6 (a)  
 308 and (b), respectively. It is clear from Fig.6 that the proposed method outperforms monostatic algorithm in  
 309 both Scenario 1 and Scenario 2 in noisy conditions, and the advantage of the proposed method over  
 310 monostatic algorithm in Scenario 2 is larger than that in Scenario 1, which coincides with the observations  
 311 in Section 4.1. It can be seen from Fig. 5 and Fig.6 that the advantage of the proposed method over  
 312 monostatic algorithm in noisy conditions is larger than that in non-noise conditions in Scenario 1, which  
 313 implies that the multi-aspect deployment has better robustness against noise than the monostatic  
 314 deployment. In addition, the classification accuracy yielded by the proposed method with 4 observation  
 315 aspects is higher than that yielded with 3 observation aspects.

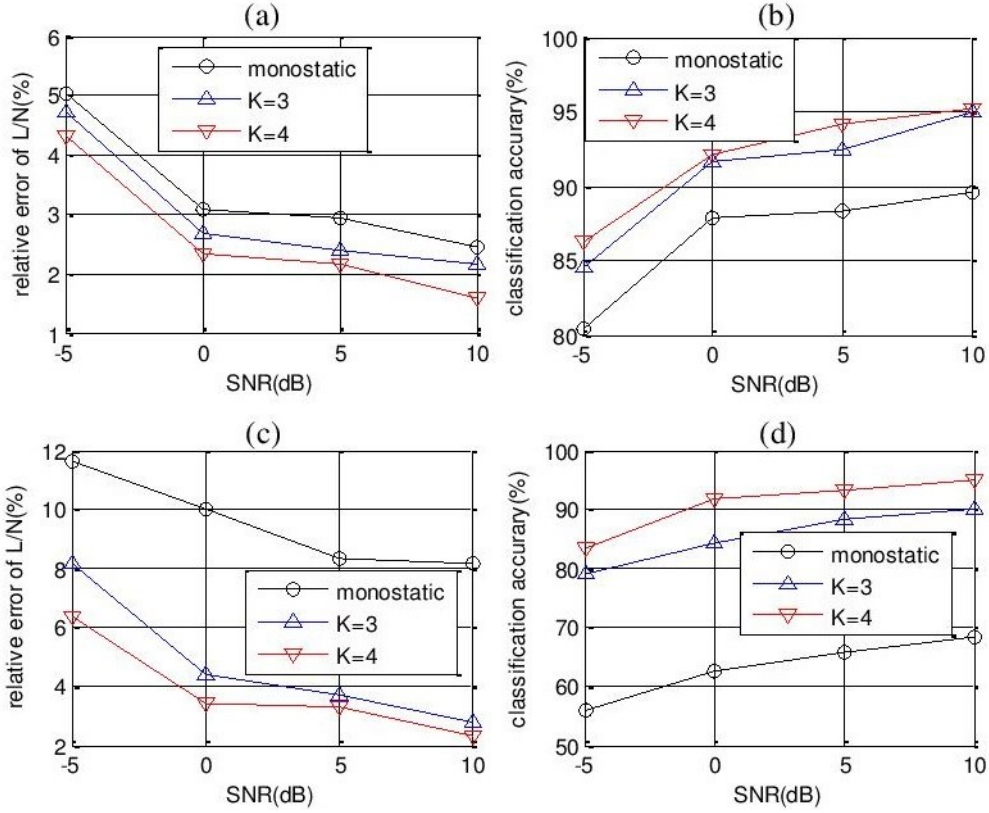


**Fig. 6.** The performances of the proposed method under different noise levels.  
a The relative estimation error of  $L/N$  quotient versus SNR when  $\beta_{los,i} \in [0^\circ, 3^\circ]$ .  
b The classification accuracy versus SNR when  $\beta_{los,i} \in [0^\circ, 3^\circ]$ .  
c The relative estimation error of  $L/N$  quotient versus SNR when  $\beta_{los,i} \in [0^\circ, 70^\circ]$ .  
d The classification accuracy versus SNR when  $\beta_{los,i} \in [0^\circ, 70^\circ]$ .

#### 4.3. Experiments with Real Data

To illustrate the proposed algorithm, real echoes from a 5-blade rotor were recorded by a frequency modulated continuous wave (FMCW) radar at the carrier frequency of 9.8 GHz with a bandwidth of 200 MHz. The rotor is rotating without translation motion and its rotational speed and blade length are 5.5 revolutions per second (rps) and 0.18 m, respectively. The rotor attitude is non-horizontal, and the azimuth angle  $\alpha_{rot}$  and pitch angle  $\beta_{rot}$  are approximately equal to  $180^\circ$  and  $80^\circ$ , respectively. In this experiment, the rotor is observed by this radar from multiple aspect angles, and the distance between the radar and the rotor is about 3 m. The pitch angles of the LOS are set much larger than  $3^\circ$  because we are aimed at applications of classifying micro-Drones in city scenarios. A diagram of the experiment setup is shown in Fig. 7 and the LOS angles are listed in Table 7.

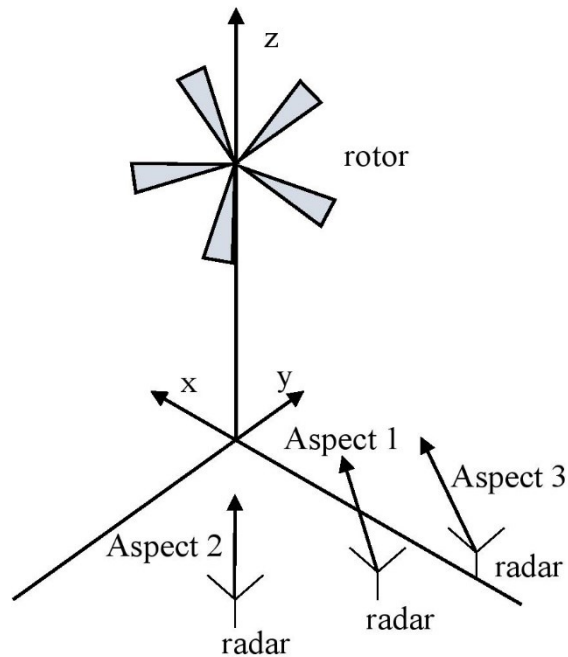
The spectrograms of the received signals at Aspect 1, 2, and 3 are shown in Figs. 8 (a), (b) and (c), respectively. We can see that the maximal Doppler shifts in Fig. 8 (a), (b) and (c) are different from each other, which are estimated as 139 Hz, 167 Hz, and 222 Hz, respectively, using the method proposed in Section 3.1. It can be seen that the received signal is periodic, and period can be approximately



337 estimated as 36ms according to the spectrogram. Considered that the number of blades is 5, the rotational  
 338 speed can be calculated as  $\omega = 1/NT \approx 5.6\text{rps}$ , which is approximately equal to the true value. It is worth  
 339 emphasizing that the intensity of the positive Doppler shift of the received signal is much stronger than  
 340 that of the negative Doppler shift, and the negative flashes of the received signal are almost buried in the  
 341 noisy, this is because the scattering coefficients of the front side of the rotor blades are much larger than  
 342 that of the rear side of the rotor blades.

343 **Table 7** The LOS angles in real data experiment

	$\alpha_{los,i}$	$\beta_{los,i}$
Aspect 1	15°	60°
Aspect 2	45°	60°
Aspect 3	0°	45°



345  
 346 **Fig. 7.** The setup of the real data experiment.  
 347

348 With the estimated maximal Doppler shifts and the configurations of the LOS angles, the proposed  
 349 algorithm is applied on the multi-aspect micro-Doppler signatures to determine the attitude angles and the  
 350  $L/N$  quotient. The resulted attitude angles are  $(171^\circ, 79^\circ)$ , and the  $L/N$  quotient is estimated to be 0.0351,  
 351 which is very close to the true value, i.e. 0.0360, with a relative error of 2.5%. The above results verify the  
 352 effectiveness of the proposed method.

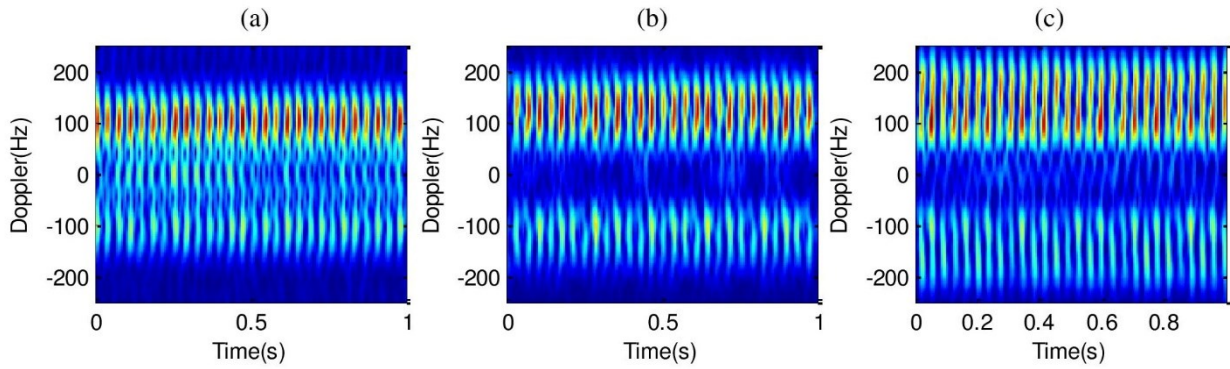


**Fig. 8.** The spectrogram of the received signal from (a) Aspect 1, (b) Aspect 2 and (c) Aspect 3.

## 5. Conclusion

In this paper, an attitude-independent  $L/N$  quotient estimation algorithm is proposed based on multi-aspect micro-Doppler signatures. The proposed algorithm is robust to the helicopter attitude and capable of estimating the  $L/N$  quotients of non-horizontal helicopters. This algorithm has significant application in helicopter classification especially in conditions of non-cooperative targets with unknown attitudes. The proposed algorithm can be divided into two stages. First, the period and maximal Doppler shift of the received signal are extracted via monostatic micro-Doppler analysis at each aspect. Secondly, the attitude angles of the target are extracted via multi-aspect micro-Doppler analysis, and the  $L/N$  quotient is calculated by using the extracted attitude angles. The extracted  $L/N$  quotient can then be used in helicopter classification. Since the proposed algorithm accomplishes attitude-independent  $L/N$  quotient estimation, the accuracy of helicopter classification yielded by the proposed algorithm is higher than that yielded by the monostatic  $L/N$  quotient estimation methods. The performance gain of the proposed method is obtained at the cost of multi-aspect observations. In possible applications, a system using distributed MIMO with joint radar and communication capabilities as the one presented in [31] would allow a cost free sharing of the estimated maximal Doppler shift and periods, therefore, be capable of performing the proposed method without additional cost. It is worth emphasizing that the  $L/N$  quotient can be jointly used with other features such as range-slow-time image [16] to further improve the classification accuracy. The robustness of the proposed algorithm with respect to the helicopter attitude is evaluated with simulations. Experiments with real data have also confirmed the effectiveness of the proposed method.

## 6. Acknowledgments

This work was supported in part by the National Natural Science Foundation of China under Grants 61422110, 41271011 and 61661130158, and in part by the National Ten Thousand Talent Program of China (Young Top-Notch Talent), and in part by the Tsinghua National Laboratory for Information Science (TNList), and in part by the Tsinghua University Initiative Scientific Research Program.

## 7. References

- [1] Chen, V. C., Li, F., Ho, S. S., *et al.*: 'Micro-Doppler effect in radar: phenomenon, model, and simulation study', IEEE Transactions on Aerospace and Electronic Systems, 2006, **42**, (1), pp. 2–21.
- [2] Björklund, S., Petersson, H., Hendeby, G.: 'Features for micro-Doppler based activity classification', IET Radar, Sonar & Navigation, 2015, **9**, (9), pp. 1181–1187.
- [3] Sparr, T., Krane, B.: 'Micro-Doppler analysis of vibrating targets in SAR', IEE Proceedings Radar, Sonar & Navigation, 2003, **150**, (4), pp. 277–283.
- [4] Lei, J., and Lu, C.: 'Target classification based on micro-Doppler signatures', IEEE International Radar Conference, Arlington, USA, May 2015, pp. 179–183.
- [5] Kim, Y., Ling, H.: 'Human activity classification based on micro-Doppler signatures using a support vector machine', IEEE Transactions on Geoscience and Remote Sensing, 2009, **47**, (5), pp. 1328–1337.
- [6] Lei, P., Sun, J., Wang, J., *et al.*: 'Micromotion parameter estimation of free rigid targets based on radar micro-Doppler', IEEE Transactions on Geoscience and Remote Sensing, 2012, **50**, (10), pp. 3776–3786.
- [7] Zhang, R., Li, G., Zhang, Y. D.: 'Micro-Doppler Interference Removal via Histogram Analysis in Time-Frequency Domain', IEEE Transactions on Aerospace and Electronic Systems, 2016, **52**, (2), pp. 755–768.
- [8] Misiurewicz, J., Kulpa, K., Czekala, Z.: 'Analysis of radar echo from a helicopter rotor hub', in Proceedings of IEEE International Conference on Microwaves and Radar, 1998, no. 3, pp. 866–870.
- [9] Thayaparan, T., Abrol, S., Riseborough, E., *et al.*: 'Analysis of radar micro-Doppler signatures from experimental helicopter and human data', IET Radar, Sonar and Navigation, 2007, **1**, (4), pp. 289–299.
- [10] Rotander, C. E., Sydow, H. V.: 'Classification of helicopters by the L/N-quoutient', in Proceedings of the Radar 97, 1997, pp. 629–633.
- [11] Muoz Ferraras, J., Perez Martinez, F., Burgos Garcia, M.: 'Helicopter classification with a high resolution LFM CW radar', IEEE Transactions on Aerospace and Electronic Systems, 2009, **45**, (4), pp. 1373–1384.
- [12] Tikkinen, J. M., Helander, E., E., Visa, A.: 'Joint utilization of incoherently and coherently integrated radar signal in helicopter categorization', in IEEE International Radar Conference, Arlington, USA, May 2005, pp. 540–545.
- [13] Costa, H., C., A., De Matos, M., C.: 'Measuring time between peaks in helicopter classification using continuous wavelet transform', in IEEE Radar Conference, Rome, Italy, May 2008, pp. 1–6.
- [14] Oh, S. R., Pathak, K., Agrawal, S. K., *et al.*: 'Approaches for a tether-guided landing of an autonomous helicopter', IEEE Transactions on Robotics, 2006, **22**, (3), pp. 536–544.
- [15] Barczyk, M., Lynch, A. F.: 'Invariant observer design for a helicopter UAV aided inertial navigation system', IEEE Transactions on Control Systems Technology, 2013, **21**, (3), pp. 791–806.
- [16] Yoon, S. H., Kim, B., Kim, Y. S.: 'Helicopter classification using time-frequency analysis', IET Electronics Letters, 2000, **36**, (22), pp. 1871–1872.

- 430 [17] Zhang, R., Li, G., Clemente, C., *et al.*: 'Helicopter classification via period estimation and time-frequency  
431 masks', In IEEE 6th International Workshop on Computational Advances in Multi-Sensor Adaptive Processing,  
432 Cancun, Mexico, Dec. 2015, pp. 61–64.
- 433 [18] Setlur, P., Ahmad, F., Amin, M.: 'Helicopter radar return analysis: Estimation and blade number selection',  
434 Signal Processing, 2011, **91**, (6), pp. 1409–1424.
- 435 [19] Gaglione, D., Clemente, C., Coutts, F., *et al.*: 'Model-based sparse recovery method for automatic classification  
436 of helicopters', In 2015 IEEE Radar Conference, Johannesburg, South Africa, Oct. 2015, pp. 1161–1165.
- 437 [20] Zhu, R. F., Zhang, Q., Zhu, X. P., *et al.*: 'Micro-Doppler analysis of vibrating target in bistatic radar', In 2nd  
438 Asian-Pacific Conference on Synthetic Aperture Radar, Xian, China, Oct. 2009, pp. 981–984.
- 439 [21] Luo, Y., He, J., Liang, X. J., *et al.*: 'Three-dimensional micro-Doppler signature extraction in MIMO radar', In  
440 2nd International Conference on Signal Processing Systems, Dalian, China, Feb. 2010, pp. V2–1.
- 441 [22] Clemente, C., Soraghan, J. J.: 'Vibrating target micro-Doppler signature in bistatic SAR with a fixed receiver',  
442 IEEE Transactions on Geoscience and Remote Sensing, 2012, **50**, (8), pp. 3219–3227.
- 443 [23] Smith, G. E., Woodbridge, K., Baker, C. J., *et al.*: 'Multistatic micro-Doppler radar signatures of personnel  
444 targets', IET Signal Processing, 2010, **4**, (3), pp. 224–233.
- 445 [24] Karabacak, C., Gürbüz, S. Z., Guldogan, M. B., *et al.*: 'Multi-aspect angle classification of human radar  
446 signatures', Proceedings of SPIE, 2013, pp. 873408–873408.
- 447 [25] Fioranelli, F., Ritchie, M., Griffiths, H.: 'Multistatic human micro-Doppler classification of armed/unarmed  
448 personnel', IET Radar, Sonar & Navigation, 2015, **9**, (7), pp. 857–865.
- 449 [26] Fairchild, D. P., Narayanan, R. M.: 'Multistatic micro-doppler radar for determining target orientation and  
450 activity classification', in IEEE Transactions on Aerospace and Electronic Systems, 2016, **52**, (1), pp. 512–521.
- 451 [27] Clemente, C., Soraghan, J. J., 'GNSS-based passive bistatic radar for micro-Doppler analysis of helicopter rotor  
452 blades', IEEE Transactions on Aerospace and Electronic Systems, 2014, **50**, (1), 491–500.
- 453 [28] Frankford, M. T., Stewart, K. B., Majurec, N., *et al.*: 'Numerical and experimental studies of target detection  
454 with MIMO radar', IEEE Transactions on Aerospace and Electronic Systems, 2014, **50**, (2), pp. 1569–1577.
- 455 [29] Baczyk, M. K., Sameczyński, P., Kulpa, K., *et al.*: 'Micro-Doppler signatures of helicopters in multistatic  
456 passive radars', IET Radar, Sonar & Navigation, 2015, **9**, (9), pp. 1276–1283.
- 457 [30] Gu, J. F., Zhu, W. P., Swamy, M. N. S.: 'Joint 2-D DOA estimation via sparse L-shaped array', IEEE  
458 Transactions on Signal Processing, 2015, **63**, (5), pp. 1171–1182.
- 459 [31] Gaglione, D., Clemente, C., Ilioudis, C. V., *et al.*: 'Fractional Fourier Based Waveform for a Joint Radar-  
460 Communication System', in IEEE International Radar Conference 2016, Philadelphia, USA, May 2016, pp. 2–16.
- 461 [32] Ritchie, M., Fioranelli, F., Borrión, H., & Griffiths, H.: 'Multistatic micro-doppler radar feature extraction for  
462 classification of unloaded/loaded micro-drones'. IET Radar, Sonar and Navigation, 2016.
- 463  
464  
465  
466  
467  
468  
469  
470  
471  
472  
473  
474  
475  
476  
477  
478